Persistent self-induced Larmor precession evidenced through periodic revivals of coherence

H. Sigurdsson,[1, 2, *] I. Gnusov,[3] S. Alyatkin,[3] L. Pickup,[2] N.A. Gippius,[3] P.G. Lagoudakis,[3, 2] and A. Askitopoulos[3, 4, †]

[1] *Science Institute, University of Iceland, Dunhagi 3, IS-107, Reykjavik, Iceland*
[2] *School of Physics and Astronomy, University of Southampton, Southampton, SO171BJ, United Kingdom*
[3] *Skolkovo Institute of Science and Technology, Bolshoy Boulevard 30, building 1, 121205 Moscow, Russia*
[4] *QUBITECH, Thessalias 10, Chalandri, Athens, Greece*

(Dated: September 2, 2022)

Interferometric measurements of an optically trapped exciton-polariton condensate reveal a regime where the condensate pseudo-spin precesses persistently within the driving optical pulse. For a single $20\,\mu$s optical pulse the condensate pseudo-spin undergoes over 10^5 full precessions with striking frequency stability. The emergence of the precession is traced to polariton non-linear interactions, that give rise to a self-induced out-of-plane magnetic field, which in turn drives the system spin dynamics. The Larmor precession frequency and trajectory is directly influenced by the condensate density, enabling the control of this effect with optical means. Our results accentuate the system's potential for the realization of magnetometry devices and can lead to the emergence of spin-squeezed polariton condensates.

Exciton-polaritons (here-forth polaritons) are two-component bosonic quasi-particles that can condense into a macroscopically occupied state [1, 2]. The system spinor order parameter is related to a pseudo-spin [3], which along with strong interparticle interactions, has enabled the observation of spin switching and hysteresis under quasi-resonant excitation [4, 5]. From the perspective of manipulating a coherent many-body state, non-resonant injection of polaritons results in some complications due to the order parameter depolarizing and dephasing due to interactions of the condensate with the background reservoir of non-condensed particles [6, 7]. However, the development of nonresonant techniques to spatially separate the reservoir and condensate [8–12] has enabled better harnessing of the condensate coherence properties and spin-degree of freedom. Today, optical trapping has revealed intriguing phenomena like spin switching, bistabilitiy, inversion and bifurcations [13–18] all under non-resonant excitation. This allowed for the proposition of polariton condensates for a number of novel spinoptronic devices, such as optoelectronic spin switches and spin valves [19, 20].

The condensate spin dynamics are strongly influenced by the anisotropic polariton interactions [21] and have revealed the existence of spin quantum beats [22], as well as a dynamic spin precession [23], which result in a self induced out of plane magnetic field [3, 24–26]. Under sub-picosecond pulsed excitation, the out-of-equilibrium nature of the system leads to a transient modification of the system non-linearity (≈ 5 ps polariton lifetime) with the precession quickly dampened. When the system is continuously driven with a resonant field, the condensate pseudo-spin is fixed by the polarization of the excitation and is not allowed to evolve in time [4]. However, under continuous wave non-resonant optical pumping where the condensate losses are continuously balanced by an external optical pump, these precession dynamics are expected to survive much longer but have, so far, not been directly observed in the pseudo-spin dynamics. Theoretical investigations [3, 24, 25, 27] as well as recent spin noise experiments [28] and second-order-correlation measurements [17] show that a precession of the condensate pseudo-spin can indeed take place, which would further underline the potential applicability of the system in fields ranging from magnetometry to coherent control on the Bloch sphere, in close analogy to atomic systems [29].

In this letter, we report the observation of a periodic partial collapse and revival of interferometric visibility in a spinor polariton condensate in the dynamic equilibrium regime. The origin of these revivals is traced to the self-induced Larmor precession of the macroscopic condensate pseudo-spin [30]. This is further evidenced by tuning the condensate density, which controls the spin precession rate, and through numerical simulations. We observe that the precession persists with prodigious stability throughout the excitation pulse duration of $20\,\mu$s, implying more than 10^5 cycles in every experimental realization with a coherence time of ~ 1 ns. As the condensate coherence time is considerably longer than the spin precession period $T_r \sim 150$ ps, the system can de-facto be described as a spin coherent state that has been suggested as a basis for polariton condensates in quantum information applications [31–33]. Despite the non-Hermitian nature of the polariton Hamiltonian, the existence of parity-time (PT) symmetry in this regime is not precluded, as has already been demonstrated in other non-Hermitian photonic systems [34, 35].

Using a non-resonant circularly polarized optical excitation scheme, we induce an optical trap on our microcavity sample [36] and perform time-delayed interferometric measurements [37]. The circular polarization of the pump induces a spin imbalance in the reservoir resulting in a dominantly co-polarized condensate above

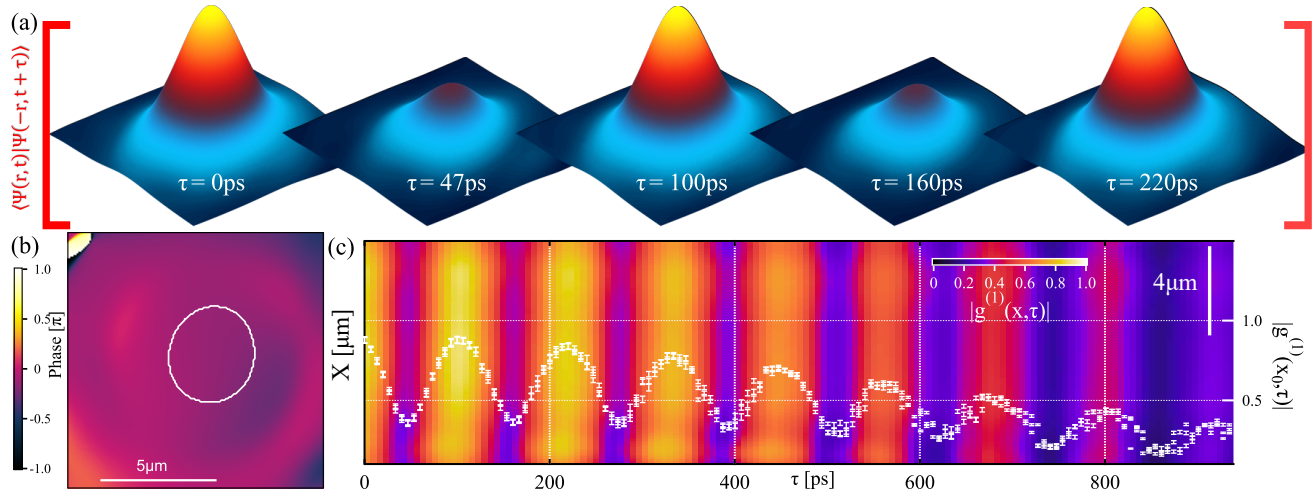

FIG. 1. (a) Condensate $|\langle\Psi^\dagger(\mathbf{r},t)\Psi(-\mathbf{r},t+\tau)\rangle|$ reconstructed through Fourier analysis for varying τ. (b) Condensate spatial phase difference $\Delta\Phi(\mathbf{r},\tau)$ for $\tau = 0$ showing a uniform phase across the whole condensate. White line indicates the condensate FWHM. (c) First order coherence function $|g^{(1)}(x,\tau)|$ versus τ and x for a central slice of the condensate. White dots are the averaged $|g^{(1)}(\tau)|$ around the peak (X_0) of the condensate plotted versus the right axis and error bars are the standard deviation.

threshold [7, 13]. Through Fourier analysis [37] of the interference fringes we then extract the spatial phase map that corresponds to the phase difference from opposite sides of the condensate $\Delta\Phi(\mathbf{r},\tau) = \Phi(\mathbf{r},t) - \Phi(-\mathbf{r},t+\tau)$ and first order coherence function,

$$g^{(1)}(\mathbf{r}_1,\mathbf{r}_2,\tau) = \frac{\langle\Psi^\dagger(\mathbf{r}_1,t)\Psi(\mathbf{r}_2,t+\tau)\rangle}{\sqrt{\langle|\Psi(\mathbf{r}_1,t)|^2\rangle\langle|\Psi(\mathbf{r}_2,t+\tau)|^2\rangle}}, \quad (1)$$

where $\Psi = (\psi_+,\psi_-)^{\mathrm{T}}$ is the condensate spinor and $\langle.\rangle = \frac{1}{T}\int_0^T dt$ denotes time averaging over the camera integration time within a single realization of the condensate, shown in Fig. 1.

Being a two-component spinor, it is convenient to define a macroscopic condensate pseudo-spin [3],

$$\mathbf{S} = \frac{1}{2}\Psi^\dagger\boldsymbol{\sigma}\Psi, \quad (2)$$

where $\boldsymbol{\sigma} = (\hat{\sigma}_x,\hat{\sigma}_y,\hat{\sigma}_z)$ is the Pauli matrix vector. The components of the pseudo-spin $\mathbf{S} = (S_x,S_y,S_z)^{\mathrm{T}}$, which correspond explicitly to the Stokes components of the emitted cavity light, are written $S_x = \mathrm{Re}(\psi_-^*\psi_+)$, $S_y = -\mathrm{Im}(\psi_-^*\psi_+)$, and $S_z = (|\psi_+|^2 - |\psi_-|^2)/2$. The total pseudo-spin is $S_0 = \sqrt{S_x^2+S_y^2+S_z^2} = (|\psi_+|^2+|\psi_-|^2)/2$. The degree of circular polarization (DCP) then corresponds to $\langle S_z\rangle/\langle S_0\rangle$.

Scanning the time delay τ we observe regular periodic oscillations of the amplitude of the condensate self-correlator ($|\langle\Psi^\dagger(\mathbf{r},t)\Psi(-\mathbf{r},t+\tau)\rangle|$), Fig. 1(a), with a periodicity of ≈ 110 ps. The phase map of the condensate shows a flat distribution within the full width half maximum (FWHM) region of the condensate for all time delays (see Supplementary Video), while the extracted first order coherence function also displays similar oscillations shown in Fig. 1(b,c). Notably, the amplitude of the revivals is almost half the coherence amplitude, indicating that the observed dynamic beating is between non-orthogonal states. The extended nanosecond coherence times of our system in this regime [6], enables us to observe up to 8 beatings over the delay range available in our configuration. The fact that we are able to observe subnanosecond coherence oscillations over such long excitation pulse duration (20 μs) evidences the condensate's frequency stability and robustness. Indeed the only available effect that can compromise the stability of the system are optical heating effects, which will slowly but steadily change the condensate energy level and polariton interaction strength. We point out that spin hysteresis effects, in the same configuration, governed by the same underlying mechanisms and limitations, have demonstrated their perseverance even up to 100's of milliseconds [15].

Performing the same experiment, but for a condensate density just above threshold ($P = 1.14P_{\mathrm{th}}$), we observe the absence of coherence revivals Fig. 2(a). As this indicates that the condensate density is a decisive factor in the emergence of the effect, we gradually increase it, thus raising the total interactions in the system. We subsequently observe the emergence of the periodic oscillations of the first order coherence function that, with increasing condensate particle number, become faster and more pronounced Fig. 2(b-d). To extract the relevant parameters of these oscillations, we approximate the first order coherence as $|g^{(1)}(\tau)| = g^{(1)}_{\mathrm{env}}(\tau)(1 - A\sin^2(\omega\tau))$, where ω and A are fitting parameters and $g^{(1)}_{\mathrm{env}}(\tau)$ represents the analytic coherence function that takes into account particle number fluctuations and the inter-particle interaction strength, described in [6, 38]. We note that in order to measure the condensate phase-coherence time

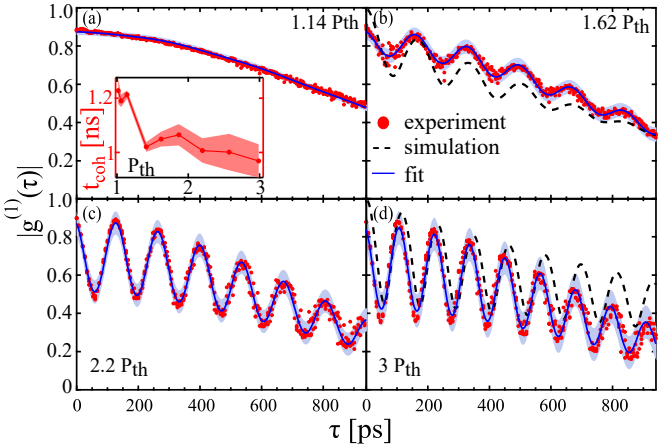

FIG. 2. $|g^{(1)}(\tau)|$ for increasing condensate density, $P = 1.14P_{\rm th}$ (a), $P = 1.62P_{\rm th}$ (b), $P = 2.2P_{\rm th}$ (c), $P = 3P_{th}$ (d). Red circles correspond to $|g^{(1)}(\tau)|$ averaged within the condensate FWHM region, continuous blue line is the fit and shaded area the 95% prediction band of the fitting parameters. Dashed black lines in (b) and (d) are the simulation results described in the text. Inset in (a) shows the extracted coherence time $t_{\rm coh}$ for increasing density.

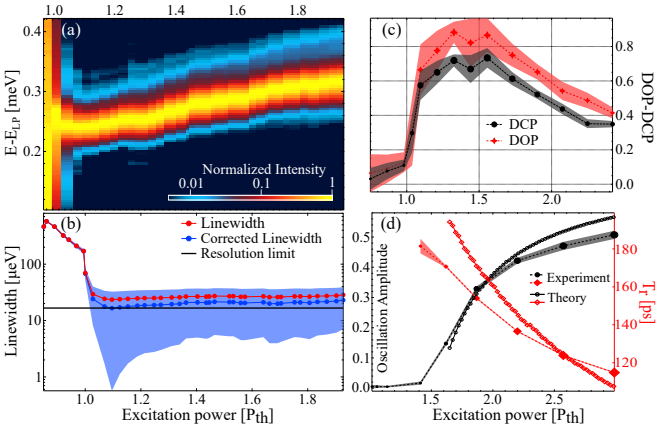

FIG. 3. (a) Condensate energy vs excitation power in units of threshold power ($P_{\rm th}$), in a logarithmic colorscale. The spectrum for each excitation power is extracted from energy dispersion imaging at zero in-plane momentum and have been intensity normalized for clarity. Condensate energy is measured relative to the zero momentum free polariton state. (b) Corresponding extracted linewidth (red dots) also taking into account resolution correction (blue dots), blue shaded region represents the error of the fit. (c) DOP and DCP of the condensate vs excitation power. (d) Oscillation amplitude (black dots, left axis) and period (red diamonds, right red axis) extracted from the fit of $|g^{(1)}(\tau)|$ and corresponding parameters from simulation (filled and open symbols respectively).

$g^{(1)}_{\rm env}(\tau)$ one needs to also account for the vectorial nature of the light field and employ a full coherence tomography approach [39, 40]. In order to limit the number of free parameters, we approximate $g^{(1)}_{\rm env}(\tau)$ with a Gaussian function that incorporates all decoherence effects into a single parameter $t_{\rm coh}$ describing the condensate coherence time [inset in Fig. 2(a)] [38] and fit the experimental $|g^{(1)}(\tau)|$ in Fig. 2(a-d). We note that the observed revivals are well approximated with this single beat frequency ω even for relatively low oscillation amplitude. This points to the presence of a coherent dual mode (two color) condensate.

We do not observe any spatial reshaping effects in $|\langle\Psi^\dagger(\mathbf{r},t)\Psi(-\mathbf{r},t+\tau)\rangle|$ that would be indicative of mixing of the ground state with higher order modes of the optical trap [41, 42]. Nevertheless, we perform a spectroscopic study of the condensate energy and linewidth. In Fig. 3(a,b) we show that even far above threshold, the potential contains a single energy mode with a resolution limited linewidth. To further verify that the observed coherence revivals originate from the precession of the condensate pseudo-spin, we record the evolution of the time-averaged DCP and degree of polarization (DOP) of our system. Just above threshold we observe a high DCP Fig. 3(c), which gradually declines after $1.5P_{\rm th}$.

The condensate DOP also starts to degrade for the same excitation power, indicating that the pseudo-spin of the condensate $\langle\mathbf{S}\rangle$ [see Eq. (2)] is not tilting towards an attractor in the equatorial plane of the Poincaré (Bloch) sphere (which would explain the drop in DCP but not DOP). This effective depolarization of the system, perfectly coincides with the emergence of the revivals of coherence. The extracted period and amplitude of the $|g^{(1)}(\tau)|$ oscillations are displayed in Fig. 3(d) for varying condensate density. The coherence oscillation amplitude sharply increases past the critical value of $1.5P_{\rm th}$, and then grows sublinearly due to the self-induced (nonlinear) nature of the effective out-of-plane magnetic field.

We can understand the dynamics of the self-induced Larmor precession by modelling the spinor polariton condensate order parameter through a set of generalized Gross-Pitaevskii equations coupled to spin-polarized rate equations describing excitonic reservoirs X_σ feeding the two spin components of the condensate,

$$i\dot{\psi}_\sigma = \eta_\sigma(t) + \frac{1}{2}\Big[\alpha|\psi_\sigma|^2 + i\left(RX_\sigma - \Gamma\right)\Big]\psi_\sigma, \tag{3a}$$

$$\dot{X}_\sigma = -\left(\Gamma_R + R|\psi_\sigma|^2\right)X_\sigma + \Gamma_s(X_{-\sigma} - X_\sigma) + P_\sigma. \tag{3b}$$

Here, $\eta_\sigma(t)$ is Gaussian stochastic noise defined by the correlators $\langle d\eta_\sigma(t)d\eta_{\sigma'}(t')\rangle = (\Gamma + RX_\sigma)\delta_{\sigma\sigma'}\delta(t-t')/2$ and $\langle d\eta_\sigma(t)d\eta^*_{\sigma'}(t')\rangle = 0$. Here, α denotes the same spin polariton-polariton interaction strength, R is the rate of stimulated scattering of polaritons into the condensate, and Γ is the polariton decay rate, Γ_R and Γ_s describe the decay rate and spin relaxation of reservoir excitons [43]. For simplicity, we neglect the polariton-reservoir interactions due to the small overlap between the trapped condensate and the pumped reservoir [37]. Such interactions would induce an additional static effective Zeeman

splitting in the condensate under an elliptically polarized pump and a weak focusing nonlinearity which did not produce any qualitatively changes to the results in the absence of in-plane anisotropy [7].

The active reservoir X_σ, which feeds the condensate, is driven by a background of inactive excitons P_σ which do not satisfy energy-momentum conservation rules to scatter into the condensate. Since these inactive excitons also experience spin relaxation Γ_s the polarization of P_σ will not coincide with that of the incident optical excitation. For the rate equation describing the inactive reservoir dynamics [37] one can derive the following steady state expression,

$$\begin{pmatrix} P_+ \\ P_- \end{pmatrix} = \frac{L}{W + 2\Gamma_s} \begin{pmatrix} W\cos^2(\theta) + \Gamma_s \\ W\sin^2(\theta) + \Gamma_s \end{pmatrix} \tag{4}$$

where L is the power of the optical excitation, θ is the quarter wave plate angle of the experiment determining the polarization of the incident light, and W is a phenomenological spin-conserving redistribution rate of inactive excitons into active excitons.

The precession of the pseudo-spin $\mathbf{S}$ naturally appears due to the parity symmetry breaking driving term $P_+ \neq P_-$ (i.e., elliptical pumping) which creates a spin imbalanced reservoir and condensate, which results in an effective Zeeman splitting of strength $\Omega_z = \alpha S_z$. It is clear that if the pseudo-spin is initially tilted with respect to the $\hat{\mathbf{z}}$ axis of the sample (direction out of the cavity plane) it will start precessing around $\mathbf{\Omega} = \Omega_z\hat{\mathbf{z}}$ due to the action of the magnetic field $\dot{\mathbf{S}} = \mathbf{\Omega} \times \mathbf{S}$. Results from simulation are shown in Fig. 2(b,d) showing good agreement with the experiment.

The unique feature of the polariton condensate is its driven-dissipative nature which, in hand with the nonlinearity α, drives the pseudo-spin always into the same orbital trajectory on the Bloch sphere for different initial conditions and fixed parameters [see Fig. 4(a)]. In other words, there exists a stable limit cycle solution [44] whose magnitude, polar angle, and period is determined by the parameters of the experiment, such as excitation strength and polarization θ. This is why the same oscillations can be observed in the $g^{(1)}(\tau)$ between different experimental realizations of the condensate (i.e., the precession is strongly reproducible). In Fig. 3(d) we plot the precession period and amplitude from simulation for circularly polarized pumping, showing a qualitative match with experiment.

We plot the simulated trajectory of the condensate pseudo-spin on a Bloch sphere, Fig. 4(a), as well as individual components, in Fig. 4(b). As the condensate density builds-up under elliptical pumping, the pseudo-spin quickly converges (within $\approx 40/\Gamma$) to a fixed periodic orbit on the Bloch sphere. The pseudo-spin long time trajectory is not found to depend on the initial condition [Fig. 4(a) solid-green and dashed-magenta lines], implying its limit cycle character. Physically, it means that the long-time trajectory is not affected by the spontaneous symmetry breaking during condensation, but each realization can have a different starting point on said trajectory. This suggests that the precession cannot be resolved through time synchronized experiments, integrating over different realizations, as every time the oscillation can have an arbitrary starting point (see Fig. 4(b) where solid and dashed lines depict the different realizations).

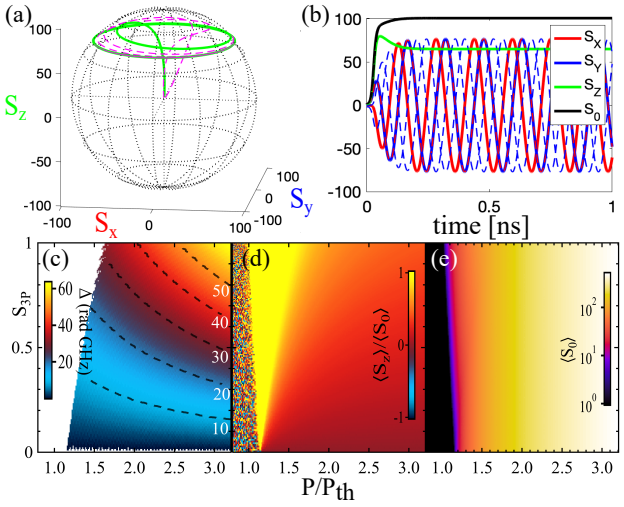

FIG. 4. (a) Simulated pseudo-spin trajectories on the Bloch sphere for different initial starting points (green and magenta dashed lines) and (b) corresponding pseudo-spin components. Precession frequency (with contour lines) (c), normalized $\langle S_z\rangle$ stokes component (d) and total density $\langle S_0\rangle$ (e) for varying power and excitation polarization from simulation. $S_{3,P} = \cos(2\theta)$ is the circular polarization of the excitation.

Simulations also reveal that the pseudo-spin trajectory will either converge to a fixed point attractor on the Bloch sphere with no oscillations (over-damped), reach a stable limit cycle (stable precession), or will undergo a damped precession eventually converging to a fixed point attractor (under-damped) [37]. Such regimes can be differentiated by detection of the condensate DOP [7]. In Fig. 4(c) we show the difference in frequency $\Delta = \omega_+ - \omega_-$ between the strongest spectral peaks belonging to $\psi_\pm$ from simulation. In Fig. 4(d) and 4(e) we show the corresponding time averaged pseudo-spin components $\langle S_z\rangle/\langle S_0\rangle$ and $\langle S_0\rangle$ respectively, where the averaging is done over a 50 ns time window. Notice the cutoff of the white area in Fig. 4(c) corresponds to the edge of the yellow area in Fig. 4(d) where the pseudo-spin becomes pinned along the z-direction (fixed point solution). The speckled region at low power in Fig. 4(d) is due to the condensate being below threshold resulting in a noisy pseudo-spin.

Assuming that each spin component is given by one spectral component, the limit cycle state corresponds to $\Delta \neq 0$ and $\langle S_{x,y}\rangle = 0$. This can be expressed analytically

by considering the ansatz,

$$\Psi = \begin{pmatrix} \psi_+ e^{-i\omega_+ t} \\ \psi_- e^{-i\omega_- t} \end{pmatrix}, \tag{5}$$

where $\omega_\sigma \in \mathbb{R}$ (quasi-equilibrium condition), $\dot{\psi_\sigma} = 0$, and $\dot{X_\sigma} = 0$. This is a limit cycle solution to Eq. (3) and can be expressed in terms of parameters of the model, $\omega_\sigma = \alpha|\psi_\sigma|^2/2$, $X_\sigma = \Gamma/R$, $|\psi_\sigma|^2 = P_\sigma/\Gamma - \Gamma_R/R$. It corresponds to a balance between gain and dissipation on a specific latitude line on the Bloch sphere of an angle $\Theta = \sin^{-1}(S_z/S_0) = \sin^{-1}\{\cos(2\theta)/[(1+2\Gamma_s/W)(1-2\Gamma\Gamma_R/RL)]\}$. A continuous real spectrum of ω_σ therefore belongs to these degenerate latitude lines in our driven-dissipative condensate, which can be tuned through the excitation circular polarization and power. The oscillation amplitude corresponding to Fig. 3(d) can be shown to be $1 - \sin(\Theta)$, and the oscillation period is $T_r = 2\pi/\Delta = 4\pi\Gamma(W + 2\Gamma_s)/[\alpha LW\cos(2\theta)]$ which agrees with experiment [Fig. 3(d)].

In conclusion, we have observed the partial collapse and revival of interferometric visibility in a spinor exciton-polariton condensate. The amplitude and period of these revivals are tunable through nonresonant pump induced spin population imbalance in the condensate. The origin of this effect is tracked to the self-induced Larmor precession of the condensate macroscopic pseudo-spin. Time integrated measurements evidence remarkable stability of the pseudo-spin precession throughout the excitation pulse duration ($20\,\mu$s) with 8 subnanosecond periods resolvable within the condensate coherence time (~ 1 ns), despite the small (5 ps) polariton lifetime. It would be interesting to use our experimental method to study temporal-mixing of quasi-degenerate (with same principal quantum number n) trapped states that have been proposed, but not experimentally observed, as a pathway towards simulating a flux qubit with polariton condensates [45, 46]. Recently, persistent temporal coherence beatings were reported in optically trapped polariton condensates due to bi-modal condensation in different trap modes [41, 42] with a period defined by the trap geometry and excitation power.

Our observations, reveal that driven exciton-polariton condensates in quasi-equilibrium can display persistent self-oscillations on the pseudo-spin Poincaré (Bloch) sphere for the duration of the quasi-CW optical excitation pulse, in-spite of short polariton lifetimes. This opens new interesting applications for polariton condensates such as optical magnetometry [29], which can be achieved using semimagnetic microcavities with strong exciton g-factor [47], or by utilizing electrical tuning of the exciton mode and polariton non-linearity [48, 49]. Moreover, it brings to the forefront intriguing possibilities, such as the creation of spin-squeezed states like in atomic condensates [50], and engineering of PT-symmetric states [51, 52].

The datasets presented in this paper are openly available from the University of Southampton repository [53].

A.A. acknowledges stimulating discussions with J.D. Töpfer, N.G. Berloff, S. Tsintzos. N.A.G. acknowledges support of RSF project 22-12-00351. P.G.L acknowledges support from UK's Engineering and Physical Sciences Research Council (EP/M025330/1, Hybrid Polaritonics). H.S. acknowledges the Icelandic Research Fund (Rannis), grant No. 217631-051.

* helg@hi.is
† aaskitopoulos@q.ubitech.eu

[1] J. Kasprzak, M. Richard, S. Kundermann, A. Baas, P. Jeambrun, J. M. J. Keeling, F. M. Marchetti, M. H. Szymańska, R. André, J. L. Staehli, V. Savona, P. B. Littlewood, B. Deveaud, and L. S. Dang, Bose-Einstein condensation of exciton polaritons., Nature **443**, 409 (2006).
[2] R. Balili, V. Hartwell, D. Snoke, L. Pfeiffer, and K. West, Bose-Einstein Condensation of Microcavity Polaritons in a Trap, Science **316**, 1007 (2007).
[3] K. V. Kavokin, I. A. Shelykh, A. V. Kavokin, G. Malpuech, and P. Bigenwald, Quantum theory of spin dynamics of exciton-polaritons in microcavities, Phys. Rev. Lett. **92**, 017401 (2004).
[4] A. Amo, T. C. H. Liew, C. Adrados, R. Houdré, E. Giacobino, A. V. Kavokin, and A. Bramati, Exciton–polariton spin switches, Nature Photonics **4**, 361 (2010).
[5] T. K. Paraïso, M. Wouters, Y. Léger, F. Morier-Genoud, and B. Deveaud-Plédran, Multistability of a coherent spin ensemble in a semiconductor microcavity, Nature Materials **9**, 655 (2010).
[6] A. Askitopoulos, L. Pickup, S. Alyatkin, A. Zasedatelev, K. G. Lagoudakis, W. Langbein, and P. G. Lagoudakis, Giant increase of temporal coherence in optically trapped polariton condensate, arXiv:1911.08981 [cond-mat, physics:physics] (2019), arXiv: 1911.08981.
[7] I. Gnusov, H. Sigurdsson, S. Baryshev, T. Ermatov, A. Askitopoulos, and P. G. Lagoudakis, Optical orientation, polarization pinning, and depolarization dynamics in optically confined polariton condensates, Phys. Rev. B **102**, 125419 (2020).
[8] A. Askitopoulos, H. Ohadi, A. V. Kavokin, Z. Hatzopoulos, P. G. Savvidis, and P. G. Lagoudakis, Polariton condensation in an optically induced two-dimensional potential, Physical Review B **88**, 041308 (2013).
[9] P. Cristofolini, A. Dreismann, G. Christmann, G. Franchetti, N. G. Berloff, P. Tsotsis, Z. Hatzopoulos, P. G. Savvidis, and J. J. Baumberg, Optical Superfluid Phase Transitions and Trapping of Polariton Condensates, Physical Review Letters **110**, 186403 (2013).
[10] R. Dall, M. D. Fraser, A. S. Desyatnikov, G. Li, S. Brodbeck, M. Kamp, C. Schneider, S. Höfling, and E. A. Ostrovskaya, Creation of Orbital Angular Momentum States with Chiral Polaritonic Lenses, Physical Review Letters **113**, 200404 (2014).
[11] A. Askitopoulos, T. C. H. Liew, H. Ohadi, Z. Hatzopoulos, P. G. Savvidis, and P. G. Lagoudakis, Robust plat-

form for engineering pure-quantum-state transitions in polariton condensates, Physical Review B **92**, 035305 (2015).
[12] D. Caputo, D. Ballarini, G. Dagvadorj, C. Sánchez Muñoz, M. De Giorgi, L. Dominici, K. West, L. N. Pfeiffer, G. Gigli, F. P. Laussy, M. H. Szymańska, and D. Sanvitto, Topological order and thermal equilibrium in polariton condensates, Nature Materials **17**, 145 (2018).
[13] H. Ohadi, A. Dreismann, Y. Rubo, F. Pinsker, Y. del Valle-Inclan Redondo, S. Tsintzos, Z. Hatzopoulos, P. Savvidis, and J. Baumberg, Spontaneous Spin Bifurcations and Ferromagnetic Phase Transitions in a Spinor Exciton-Polariton Condensate, Physical Review X **5**, 031002 (2015).
[14] A. Askitopoulos, K. Kalinin, T. C. H. Liew, P. Cilibrizzi, Z. Hatzopoulos, P. G. Savvidis, N. G. Berloff, and P. G. Lagoudakis, Nonresonant optical control of a spinor polariton condensate, Physical Review B **93**, 205307 (2016).
[15] L. Pickup, K. Kalinin, A. Askitopoulos, Z. Hatzopoulos, P. Savvidis, N. Berloff, and P. Lagoudakis, Optical Bistability under Nonresonant Excitation in Spinor Polariton Condensates, Physical Review Letters **120**, 225301 (2018).
[16] Y. del Valle-Inclan Redondo, H. Sigurdsson, H. Ohadi, I. A. Shelykh, Y. G. Rubo, Z. Hatzopoulos, P. G. Savvidis, and J. J. Baumberg, Observation of inversion, hysteresis, and collapse of spin in optically trapped polariton condensates, Physical Review B **99**, 165311 (2019).
[17] S. Baryshev, A. Zasedatelev, H. Sigurdsson, I. Gnusov, J. D. Töpfer, A. Askitopoulos, and P. G. Lagoudakis, Engineering photon statistics in a spinor polariton condensate, Phys. Rev. Lett. **128**, 087402 (2022).
[18] Y. C. Balas, E. S. Sedov, G. G. Paschos, Z. Hatzopoulos, H. Ohadi, A. V. Kavokin, and P. G. Savvidis, Stochastic single-shot polarization pinning of polariton condensate at high temperatures, Phys. Rev. Lett. **128**, 117401 (2022).
[19] A. Dreismann, H. Ohadi, Y. del Valle-Inclan Redondo, R. Balili, Y. G. Rubo, S. I. Tsintzos, G. Deligeorgis, Z. Hatzopoulos, P. G. Savvidis, and J. J. Baumberg, A sub-femtojoule electrical spin-switch based on optically trapped polariton condensates, Nature Materials **15**, 1074 (2016).
[20] A. Askitopoulos, A. V. Nalitov, E. S. Sedov, L. Pickup, E. D. Cherotchenko, Z. Hatzopoulos, P. G. Savvidis, A. V. Kavokin, and P. G. Lagoudakis, All-optical quantum fluid spin beam splitter, Physical Review B **97**, 235303 (2018).
[21] M. D. Martín, G. Aichmayr, L. Viña, and R. André, Polarization Control of the Nonlinear Emission of Semiconductor Microcavities, Physical Review Letters **89**, 077402 (2002).
[22] P. Renucci, T. Amand, X. Marie, P. Senellart, J. Bloch, B. Sermage, and K. V. Kavokin, Microcavity polariton spin quantum beats without a magnetic field: A manifestation of Coulomb exchange in dense and polarized polariton systems, Physical Review B **72**, 075317 (2005).
[23] A. A. Demenev, Y. V. Grishina, A. V. Larionov, N. A. Gippius, C. Schneider, S. Höfling, and V. D. Kulakovskii, Polarization instability and the nonlinear internal josephson effect in cavity polariton condensates generated in an excited state in gaas microcavities of lowered symmetry, Phys. Rev. B **96**, 155308 (2017).
[24] I. Shelykh, G. Malpuech, K. V. Kavokin, A. V. Kavokin, and P. Bigenwald, Spin dynamics of interacting exciton polaritons in microcavities, Physical Review B **70**, 115301 (2004).
[25] F. P. Laussy, I. A. Shelykh, G. Malpuech, and A. Kavokin, Effects of Bose-Einstein condensation of exciton polaritons in microcavities on the polarization of emitted light, Physical Review B **73**, 035315 (2006).
[26] D. D. Solnyshkov, I. A. Shelykh, M. M. Glazov, G. Malpuech, T. Amand, P. Renucci, X. Marie, and A. V. Kavokin, Nonlinear effects in spin relaxation of cavity polaritons, Semiconductors **41**, 1080 (2007).
[27] G. Li, T. C. H. Liew, O. A. Egorov, and E. A. Ostrovskaya, Incoherent excitation and switching of spin states in exciton-polariton condensates, Physical Review B **92**, 064304 (2015).
[28] I. I. Ryzhov, V. O. Kozlov, N. S. Kuznetsov, I. Y. Chestnov, A. V. Kavokin, A. Tzimis, Z. Hatzopoulos, P. G. Savvidis, G. G. Kozlov, and V. S. Zapasskii, Spin noise signatures of the self-induced Larmor precession, Physical Review Research **2**, 022064 (2020).
[29] D. Budker and M. Romalis, Optical magnetometry, Nature Physics **3**, 227 (2007).
[30] D. N. Krizhanovskii, D. Sanvitto, I. A. Shelykh, M. M. Glazov, G. Malpuech, D. D. Solnyshkov, A. Kavokin, S. Ceccarelli, M. S. Skolnick, and J. S. Roberts, Rotation of the plane of polarization of light in a semiconductor microcavity, Physical Review B **73**, 073303 (2006).
[31] T. Byrnes, K. Wen, and Y. Yamamoto, Macroscopic quantum computation using Bose-Einstein condensates, Physical Review A **85**, 040306 (2012).
[32] Á. Cuevas, J. C. López Carreño, B. Silva, M. De Giorgi, D. G. Suárez-Forero, C. Sánchez Muñoz, A. Fieramosca, F. Cardano, L. Marrucci, V. Tasco, G. Biasiol, E. del Valle, L. Dominici, D. Ballarini, G. Gigli, P. Mataloni, F. P. Laussy, F. Sciarrino, and D. Sanvitto, First observation of the quantized exciton-polariton field and effect of interactions on a single polariton, Science Advances **4**, 10.1126/sciadv.aao6814 (2018).
[33] S. Ghosh and T. C. H. Liew, Quantum computing with exciton-polariton condensates, npj Quantum Information **6**, 1 (2020).
[34] Y. Lumer, Y. Plotnik, M. C. Rechtsman, and M. Segev, Nonlinearly induced *pt* transition in photonic systems, Phys. Rev. Lett. **111**, 263901 (2013).
[35] R. El-Ganainy, K. G. Makris, M. Khajavikhan, Z. H. Musslimani, S. Rotter, and D. N. Christodoulides, Non-Hermitian physics and PT symmetry, Nature Physics **14**, 11 (2018).
[36] P. Cilibrizzi, A. Askitopoulos, M. Silva, F. Bastiman, E. Clarke, J. M. Zajac, W. Langbein, and P. G. Lagoudakis, Polariton condensation in a strain-compensated planar microcavity with InGaAs quantum wells, Applied Physics Letters **105**, 191118 (2014).
[37] See Supplemental Material for additional information which includes references [54–56].
[38] D. M. Whittaker and P. R. Eastham, Coherence properties of the microcavity polariton condensate, EPL (Europhysics Letters) **87**, 27002 (2009).
[39] J. Tervo, T. Setälä, and A. T. Friberg, Degree of coherence for electromagnetic fields, Optics Express **11**, 1137 (2003).
[40] L.-P. Leppänen, A. T. Friberg, and T. Setälä, Tem-

poral electromagnetic degree of coherence and Stokes-parameter modulations in Michelson's interferometer, Applied Physics B **122**, 32 (2016).

[41] K. Orfanakis, A. F. Tzortzakakis, D. Petrosyan, P. G. Savvidis, and H. Ohadi, Ultralong temporal coherence in optically trapped exciton-polariton condensates, Phys. Rev. B **103**, 235313 (2021).

[42] J. D. Töpfer, H. Sigurdsson, S. Alyatkin, and P. G. Lagoudakis, Lotka-volterra population dynamics in coherent and tunable oscillators of trapped polariton condensates, Phys. Rev. B **102**, 195428 (2020).

[43] Parameters in simulation: $\Gamma = \Gamma_R = 0.2$ ps^{-1}, $\alpha = 0.003\Gamma$, $R = 0.0075\Gamma$, $\Gamma_s = \Gamma/2$, $W = 0.385\Gamma$.

[44] R. Ruiz-Sánchez, R. Rechtman, and Y. G. Rubo, Autonomous chaos of exciton-polariton condensates, Phys. Rev. B **101**, 155305 (2020).

[45] Y. Xue, I. Chestnov, E. Sedov, S. Schumacher, X. Ma, and A. Kavokin, Split-ring polariton condensates as macroscopic two-level quantum systems, arXiv:1907.00383 [cond-mat, physics:quant-ph] (2020).

[46] E. Sedov, V. Lukoshkin, V. Kalevich, Z. Hatzopoulos, P. Savvidis, and A. Kavokin, Persistent Currents in Half-Moon Polariton Condensates, ACS Photonics **7**, 1163 (2020).

[47] J.-G. Rousset, B. Piętka, M. Król, R. Mirek, K. Lekenta, J. Szczytko, W. Pacuski, and M. Nawrocki, Magnetic field effect on the lasing threshold of a semimagnetic polariton condensate, Physical Review B **96**, 125403 (2017).

[48] G. Christmann, A. Askitopoulos, G. Deligeorgis, Z. Hatzopoulos, S. I. Tsintzos, P. G. Savvidis, and J. J. Baumberg, Oriented polaritons in strongly-coupled asymmetric double quantum well microcavities, Applied Physics Letters **98**, 081111 (2011).

[49] S. Tsintzos, A. Tzimis, G. Stavrinidis, A. Trifonov, Z. Hatzopoulos, J. Baumberg, H. Ohadi, and P. Savvidis, Electrical Tuning of Nonlinearities in Exciton-Polariton Condensates, Physical Review Letters **121**, 037401 (2018).

[50] T. Laudat, V. Dugrain, T. Mazzoni, M.-Z. Huang, C. L. G. Alzar, A. Sinatra, P. Rosenbusch, and J. Reichel, Spontaneous spin squeezing in a rubidium BEC, New Journal of Physics **20**, 073018 (2018).

[51] I. Y. Chestnov, S. S. Demirchyan, A. P. Alodjants, Y. G. Rubo, and A. V. Kavokin, Permanent Rabi oscillations in coupled exciton-photon systems with PT -symmetry, Scientific Reports **6**, 19551 (2016).

[52] P. A. Kalozoumis, G. M. Nikolopoulos, and D. Petrosyan, Coherent population oscillations and an effective spin-exchange interaction in a symmetric polariton mixture, EPL **129**, 37003 (2020).

[53] 10.5258/SOTON/D2350.

[54] G. Tosi, *Optical manipulation of quantum fluids in semiconductor microcavities*, Ph.D. thesis, Universidad Autónoma de Madrid (2013).

[55] M. Born and E. Wolf, *Principles of Optics: Electromagnetic Theory of Propagation, Interference and Diffraction of Light* (Cambridge University Press, Cambridge, 1999).

[56] K. Lagoudakis, *The Physics of Exciton-Polariton Condensates* (EPFL Press, Lausanne, 2013).